Observation of Low-Energy Metal−Metal-to-Ligand Charge Transfer Absorption and Emission: Electronic Spectroscopy of Cyclometalated Platinum(II) Complexes with Isocyanide Ligands

Siu-Wai Lai, Hiu-Wah Lam, Wei Lu, Kung-Kai Cheung, and Chi-Ming Che*

Department of Chemistry and HKU−CAS Joint Laboratory on New Materials, The University of Hong Kong, Pokfulam Road, Hong Kong

Received July 16, 2001

A series of luminescent mononuclear [(C^N^N)Pt(C≡NR)]X (HC^N^N = 6-phenyl-2,2′-bipyridine; R = ^{t}Bu (**1**), ^{n}Bu (**2**), ^{i}Pr (**3**), cyclohexyl (Cy, **4**), X = ClO_4; R = 2,6-$Me_2C_6H_3$ (Ar′, **5**), X = PF_6) and [(C^N^N)Pt(CO)]CF_3SO_3 (**6**(CF_3SO_3)) and binuclear [{(C^N^N)Pt}$_2$(μ-C≡N$(CH_2)_3$N≡C)]$(PF_6)_2$ (**7**$(PF_6)_2$) complexes were synthesized, and their spectroscopic and photophysical properties have been investigated. The crystal lattices of **1**(ClO_4) and **5**(PF_6) reveal close [C^N^N] $\pi-\pi$ intermolecular contacts (3.4−3.6 Å). Additional metal−metal interactions are evident in **5**(PF_6) with intermolecular Pt−Pt distances of 3.3831(9) Å. At complex concentration greater than 5×10^{-3} mol dm^{-3}, the UV−vis absorption spectrum of **2** displays a weak shoulder at 511 nm ($\epsilon = 120$ dm^3 mol^{-1} cm^{-1}), which does not obey Beer's law. A metal−metal-to-ligand charge transfer (MMLCT) [dσ*(Pt−Pt) → π*(C^N^)] absorption of a dimeric species via 2[Pt(C^N^N)(C≡N^{n}Bu)]$^+$ ⇌ [(C^N^N)Pt(C≡N^{n}Bu)]$_2^{2+}$ is proposed. The room-temperature emission spectrum of **4** for complex concentrations ≥ 7×10^{-3} mol dm^{-3} shows a low-energy band at 710 nm originating from a ^{3}MMLCT excited state. A corresponding well-defined low-energy absorption at 500 nm in the excitation spectrum of **4** (λ_{em} 710 nm) is assigned to the ^{1}MMLCT transition. The 77 K emissions of complexes **1**−**6** in glassy solutions are sensitive to complex concentration. Upon increasing concentrations from 5×10^{-5} to 2×10^{-3} mol dm^{-3} for **1**−**4**, red emissions at 600−625 nm ascribed to $\pi-\pi$ excimeric excited states develop at the expense of the vibronic ^{3}MLCT emissions at λ_{max} ∼502 nm. Complexes **2** and **4** show additional low-energy emissions at 739 and 710 nm, respectively, attributable to ^{3}MMLCT states. Concentrated 77 K glassy solutions of complexes **5**−**7** exhibit ^{3}MMLCT emissions (λ_{max} 711−744 nm). The broad structureless solid-state luminescence of **2**(ClO_4), **3**(ClO_4), **5**(PF_6), **6**(CF_3SO_3), and **7**$(PF_6)_2$ at 298 K (λ_{max} 701−748 nm) and 77 K (λ_{max} 744−813 nm) are assigned to ^{3}MMLCT excited states arising from intermolecular stacking interactions in the solid state. The spectroscopic properties of the related [(C^N^C)Pt(L)] (HC^N^CH = 2,6-diphenylpyridine; L = CO and C≡NAr′) solids are compared, and no MMLCT emission is evident.

Downloaded by CARLI CONSORTIUM on June 29, 2009
Published on December 11, 2001 on http://pubs.acs.org | doi: 10.1021/om0106276

Introduction

Luminescent square-planar platinum(II) complexes have received intense scrutiny with regard to characterization of the excited states and applications as chemical sensors[1,2] and photocatalysts.[3] In particular, the binuclear derivative $[Pt_2(\mu\text{-}P_2O_5H_2)_4]^{4-}$ undergoes intriguing photochemical reactions via the triplet [dσ*, pσ] excited state originating from substantial metal−metal interaction.[3c] Such interaction is also well-documented in the binuclear $[Rh_2$(1,3-diisocyanopropane)$_4]^{2+}$ system[4] and leads to shifting of the lowest energy metal-centered absorption to the visible region. Platinum(II) diimine solids exhibit unusual colors, strong emission, and highly anisotropic properties as a result of intermolecular stacking interactions.[5] Similarly, the propensity for $[Pt^{II}(tpy)X]^{n+}$ (tpy = terpyridine) derivatives to oligomerize has been extensively investigated,[6] and such processes were found to give low-energy triplet emissions in the 600−750 nm region. To account for these phenomena, Miskowski[5b] proposed oligomeric metal−metal-to-ligand charge transfer (MMLCT: dσ* → π*) and excimeric ligand-to-ligand (π → π*) excited states (Figure 1). A series of discrete d^8−d^8 complexes, namely, [{Pt(tpy)}$_2$(μ-L)]$^{n+}$ (L = bidentate ligand)[7] and [{Pt(C^N^N)}$_2$(μ-L)]$^{n+}$ (HC^N^N = 6-phen-

* Corresponding author. Fax: +852 2857 1586. E-mail: cmche@hku.hk.

(1) (a) Liu, H. Q.; Peng, S. M.; Che, C. M. *J. Chem. Soc., Chem. Commun.* **1995**, 509. (b) Liu, H. Q.; Cheung, T. C.; Che, C. M. *Chem. Commun.* **1996**, 1039. (c) Wu, L. Z.; Cheung, T. C.; Che, C. M.; Cheung, K. K.; Lam, M. H. W. *Chem. Commun.* **1998**, 1127. (d) Wong, K. H.; Chan, M. C. W.; Che, C. M. *Chem. Eur. J.* **1999**, *5*, 2845.

(2) (a) Peyratout, C. S.; Aldridge, T. K.; Crites, D. K.; McMillin, D. R. *Inorg. Chem.* **1995**, *34*, 4484. (b) Kaiwar, S. P.; Vodacek, A.; Blough, N. V.; Pilato, R. S. *J. Am. Chem. Soc.* **1997**, *119*, 3311. (c) Kunugi, Y.; Mann, K. R.; Miller, L. L.; Exstrom, C. L. *J. Am. Chem. Soc.* **1998**, *120*, 589.

(3) (a) Houlding, V. H.; Frank, A. J. *Inorg. Chem.* **1985**, *24*, 3664. (b) Sandrini, D.; Maestri, M.; Balzani, V.; Chassot, L.; von Zelewsky, A. *J. Am. Chem. Soc.* **1987**, *109*, 7720. (c) Roundhill, D. M.; Gray, H. B.; Che, C. M. *Acc. Chem. Res.* **1989**, *22*, 55. (d) Cummings, S. D.; Eisenberg, R. *J. Am. Chem. Soc.* **1996**, *118*, 1949. (e) Connick, W. B.; Gray, H. B. *J. Am. Chem. Soc.* **1997**, *119*, 11620. (f) Maruyama, T.; Yamamoto, T. *J. Phys. Chem. B* **1997**, *101*, 3806. (g) Hissler, M.; McGarrah, J. E.; Connick, W. B.; Geiger, D. K.; Cummings, S. D.; Eisenberg, R. *Coord. Chem. Rev.* **2000**, *208*, 115.

(4) (a) Rice, S. F.; Gray, H. B. *J. Am. Chem. Soc.* **1981**, *103*, 1593. (b) Rice, S. F.; Miskowski, V. M.; Gray, H. B. *Inorg. Chem.* **1988**, *27*, 4704.

10.1021/om0106276 CCC: $22.00 © 2002 American Chemical Society
Publication on Web 12/11/2001

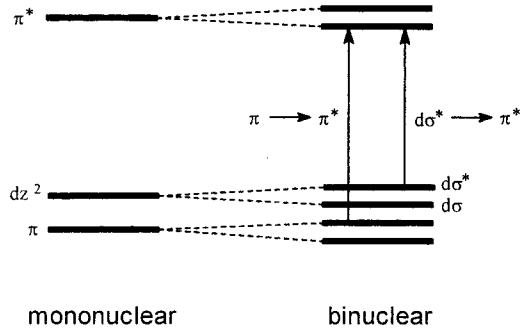

Figure 1. Schematic molecular orbital diagram illustrating d^8-d^8 and $\pi-\pi$ interactions in binuclear platinum(II) polypyridine complexes.

yl-2,2′-bipyridine),[8] have been prepared to model the low-energy [$d\sigma^*(dz^2(Pt)) \rightarrow \pi^*$(diimine)] and excimeric ligand-to-ligand emissions. However, even for those binuclear derivatives with Pt−Pt distances less than 3.0 Å, a well-defined low-energy MMLCT band like the [$(n)d\sigma^* \rightarrow (n+1)p\sigma$] transition of $[Pt_2(\mu\text{-}P_2O_5H_2)_4]^{4-}$ [3c] and $[Rh_2(1,3\text{-diisocyanopropane})_4]^{2+}$ [4] has not been observed in the absorption spectra in fluid solution at ambient temperature.

Our earlier studies on Pt(II) derivatives bearing cyclometalated 6-phenyl-2,2′-bipyridine[8,9] revealed interesting photophysical properties, including distinctive low-energy emissions in fluid solution. However, assignment of these low-energy emissions to ^{3}MMLCT excited states is complicated by the fact that the excimeric ligand-to-ligand emissions occur at a region similar to the low-energy emission of the $[\{Pt(C\text{^}N\text{^}N)\}_2(\mu\text{-}L)]^{n+}$ complexes. Here we describe the preparation of a class of derivatives bearing isocyanide and carbonyl ligands and demonstrate the effect of these auxiliaries upon metal−metal and $\pi-\pi$ interactions and photophysical properties. Comparing to the phosphine ligands such as triphenylphosphine, the less bulky isocyanide ligand leads to observation of a well-defined low-energy absorption band that can be assigned to the ^{1}MMLCT absorption by measuring the excitation spectrum of a highly concentrated CH_3CN solution ($\geq 7 \times 10^{-3}$ mol dm^{-3}) of $[(C\text{^}N\text{^}N)Pt(C{\equiv}NCy)]^+$ at ambient temperature. In addition, by employing the sterically undemanding carbonyl auxiliary, we have detected the ^{1}MMLCT transition for the newly synthesized $[(C\text{^}N\text{^}N)Pt(CO)]^+$ derivative. Lastly, differences in the spectral features of the cationic $[(C\text{^}N\text{^}N)Pt(L)]^+$ (L = C≡NAr′ and CO) complexes described in this work compared with that of the neutral [(C^N^C)Pt(L)] congeners (HC^N^CH = 2,6-diphenylpyridine) are highlighted and evaluated.

Experimental Section

General Procedures. All starting materials were used as received. 6-Phenyl-2,2′-bipyridine (HC^N^N),[10] [(C^N^N)PtCl],[9c,11] and 1,3-diisocyanopropane[12] were prepared by literature methods. Syntheses of $[(C\text{^}N\text{^}N)Pt(C{\equiv}N^tBu)]ClO_4$ (**1**(ClO_4)),[13] [(C^N^C)Pt(CO)],[14] and [(C^N^C)Pt{C≡N(2,6-$Me_2C_6H_3$)}][15] were described previously. (**Caution**: perchlorate salts are potentially explosive and should be handled with care and in small amounts.) Dichloromethane for photophysical studies was washed with concentrated sulfuric acid, 10% sodium hydrogen carbonate, and water, dried by calcium chloride, and distilled over calcium hydride. Acetonitrile for photophysical measurements was distilled over potassium permanganate and calcium hydride. All other solvents were of analytical grade and purified according to conventional methods.[16]

Fast atom bombardment (FAB) mass spectra were obtained on a Finnigan Mat 95 mass spectrometer. ^{1}H (300 MHz) and ^{13}C (126 MHz) NMR spectra were recorded on DPX 300 and 500 Bruker FT-NMR spectrometers, respectively, with chemical shift (in ppm) relative to tetramethylsilane. Elemental analysis was performed by the Institute of Chemistry at the Chinese Academy of Sciences, Beijing. Infrared spectra were recorded in Nujol on a BIO RAD FT-IR spectrophotometer. UV−vis spectra were recorded on a Perkin-Elmer Lambda 19 UV/vis spectrophotometer.

Emission and Lifetime Measurements. Steady-state emission spectra were recorded on a SPEX 1681 Fluorolog-2 series F111AI spectrophotometer. Low-temperature (77 K) emission spectra for glasses and solid-state samples were recorded in 5 mm diameter quartz tubes which were placed in a liquid nitrogen Dewar equipped with quartz windows. The emission spectra were corrected for monochromator and photomultiplier efficiency and for xenon lamp stability.

Emission lifetime measurements were performed with a Quanta Ray DCR-3 pulsed Nd:YAG laser system (pulse output 355 nm, 8 ns). The emission signals were detected by a Hamamatsu R928 photomultiplier tube and recorded on a Tektronix model 2430 digital oscilloscope. Errors for λ values (±1 nm), τ (±10%), and ϕ (±10%) are estimated. Details of emission quantum yield determinations using the method of Demas and Crosby[17] have been provided previously.[9a]

Downloaded by CARLI CONSORTIUM on June 29, 2009
Published on December 11, 2001 on http://pubs.acs.org | doi: 10.1021/om0106276

(5) (a) Kunkely, H.; Vogler, A. *J. Am. Chem. Soc.* **1990**, *112*, 5625. (b) Miskowski, V. M.; Houlding, V. H. *Inorg. Chem.* **1991**, *30*, 4446. (c) Houlding, V. H.; Miskowski, V. M. *Coord. Chem. Rev.* **1991**, *111*, 145. (d) Wan, K. T.; Che, C. M.; Cho, K. C. *J. Chem. Soc., Dalton Trans.* **1991**, 1077. (e) Miskowski, V. M.; Houlding, V. H.; Che, C. M.; Wang, Y. *Inorg. Chem.* **1993**, *32*, 2518. (f) Kato, M.; Kosuge, C.; Morii, K.; Ahn, J. S.; Kitagawa, H.; Mitani, T.; Matsushita, M.; Kato, T.; Yano, S.; Kimura, M. *Inorg. Chem.* **1999**, *38*, 1638.

(6) (a) Jennette, K. W.; Gill, J. T.; Sadownick, J. A.; Lippard, S. J. *J. Am. Chem. Soc.* **1976**, *98*, 6159. (b) Yip, H. K.; Cheng, L. K.; Cheung K. K.; Che, C. M. *J. Chem. Soc., Dalton Trans.* **1993**, 2933. (c) Aldridge, T. K.; Stacy, E. M.; McMillin, D. R. *Inorg. Chem.* **1994**, *33*, 722. (d) Bailey, J. A.; Hill, M. G.; Marsh, R. E.; Miskowski, V. M.; Schaefer, W. P.; Gray, H. B. *Inorg. Chem.* **1995**, *34*, 4591. (e) Hill, M. G.; Bailey, J. A.; Miskowski, V. M.; Gray, H. B. *Inorg. Chem.* **1996**, *35*, 4585. (f) Büchner, R.; Field, J. S.; Haines, R. J.; Cunningham, C. T.; McMillin, D. R. *Inorg. Chem.* **1997**, *36*, 3952. (g) Arena, G.; Calogero, G.; Campagna, S.; Scolaro, L. M.; Ricevuto, V.; Romeo, R. *Inorg. Chem.* **1998**, *37*, 2763. (h) Büchner, R.; Cunningham, C. T.; Field, J. S.; Haines, R. J.; McMillin, D. R.; Summerton, G. C. *J. Chem. Soc., Dalton Trans.* **1999**, 711.

(7) (a) Ratilla, E. M. A.; Scott, B. K.; Moxness, M. S.; Kostic, N. M. *Inorg. Chem.* **1990**, *29*, 918. (b) Yip, H. K.; Che, C. M.; Zhou, Z. Y.; Mak, T. C. W. *J. Chem. Soc., Chem Commun.* **1992**, 1369. (c) Bailey, J. A.; Miskowski, V. M.; Gray, H. B. *Inorg. Chem.* **1993**, *32*, 369.

(8) Lai, S. W.; Chan, M. C. W.; Cheung, T. C.; Peng, S. M.; Che, C. M. *Inorg. Chem.* **1999**, *38*, 4046.

(9) (a) Chan, C. W.; Lai, T. F.; Che, C. M.; Peng, S. M. *J. Am. Chem. Soc.* **1993**, *115*, 11245. (b) Chan, C. W.; Cheng, L. K.; Che, C. M. *Coord. Chem. Rev.* **1994**, *132*, 87. (c) Cheung, T. C.; Cheung, K. K.; Peng, S. M.; Che, C. M. *J. Chem. Soc., Dalton Trans.* **1996**, 1645. (d) Tse, M. C.; Cheung, K. K.; Chan, M. C. W.; Che, C. M. *Chem. Commun.* **1998**, 2295.

(10) Kröhnke, F. *Synthesis* **1976**, 1.

(11) Constable, E. C.; Henney, R. P. G.; Leese, T. A.; Tocher, D. A. *J. Chem. Soc., Chem. Commun.* **1990**, 513.

(12) Weber, W. P.; Gokel, G. W.; Ugi, I. K. *Angew. Chem., Int. Ed. Engl.* **1972**, *11*, 530.

(13) Lai, S. W.; Chan, M. C. W.; Cheung, K. K.; Che, C. M. *Organometallics* **1999**, *18*, 3327.

(14) Cave, G. W. V.; Fanizzi, F. P.; Deeth, R. J.; Errington, W.; Rourke, J. P. *Organometallics* **2000**, *19*, 1355.

(15) Lu, W.; Chan, M. C. W.; Cheung, K. K.; Che, C. M. *Organometallics* **2001**, *20*, 2477.

(16) Perrin, D. D.; Armarego, W. L. F.; Perrin, D. R. *Purification of Laboratory Chemicals*, 2nd ed.; Pergamon: Oxford, 1980.

(17) Demas, J. N.; Crosby, G. A. *J. Phys. Chem.* **1971**, *75*, 991.

Downloaded by CARLI CONSORTIUM on June 29, 2009
Published on December 11, 2001 on http://pubs.acs.org | doi: 10.1021/om0106276

Synthesis. [(C^N^N)Pt(C≡NR)]ClO_4 (2−4(ClO_4); R = ^{n}Bu (2), ^{i}Pr (3), Cy (4)). The methodology for the previously reported isocyanide complexes for R = ^{t}Bu (**1**(ClO_4)) was adopted.[13] To an orange suspension of [(C^N^N)PtCl] (0.10 g, 0.22 mmol) in acetonitrile (20 mL) at room temperature was added excess isocyanide, RN≡C (0.96 mmol). Upon stirring, the color of the mixture changed to cloudy orange-red, then clear red after 30 min. Addition of excess $LiClO_4$ in acetonitrile followed by diethyl ether yielded a red precipitate, which was collected and dried. Recrystallization by slow diffusion of diethyl ether into an acetonitrile solution of the crude product afforded a crystalline solid.

2(ClO_4): purple solid. Yield: 0.10 g, 76%. Anal. Calcd for $C_{21}H_{20}N_3O_4ClPt$: C, 41.42; H, 3.31; N, 6.90. Found: C, 41.06; H, 3.16; N, 6.81. FAB-MS: *m*/*z* 509 [M^+]. ^{1}H NMR (DMSO-d_6): 1.01 (t, 3H, *J* = 7.4 Hz, CH_3), 1.49 (sextet, 2H, *J* = 7.4 Hz, $(CH_2)_2CH_2CH_3$), 1.83 (quintet, 2H, *J* = 7.2 Hz, $CH_2CH_2CH_2CH_3$), 4.04 (t, 2H, *J* = 6.8 Hz, $CH_2(CH_2)_2CH_3$), 6.88 (d, 1H, *J* = 7.4 Hz), 6.97 (t, 1H, *J* = 7.4 Hz), 7.07 (t, 1H, *J* = 7.5 Hz), 7.45 (d, 1H, *J* = 7.7 Hz), 7.75−7.78 (m, 1H), 7.84 (d, 1H, *J* = 7.6 Hz), 8.01−8.06 (m, 2H), 8.31−8.33 (m, 2H), 8.56 (d, 1H, *J* = 5.1 Hz). ^{13}C{^{1}H} NMR (DMSO-d_6): 13.0, 19.1, 29.9, 44.4 (^{n}Bu), 120.2, 120.3, 124.7, 125.6, 126.0, 129.1, 131.7, 136.3, 137.5, 141.4, 142.8, 146.4, 152.4, 154.5, 156.2, 163.6, Pt-*C*N^{n}Bu not resolved. IR (Nujol): *ν* 2220 (C≡N), 1601 (C═N) cm^{-1}.

3(ClO_4): purple solid. Yield: 0.09 g, 70%. Anal. Calcd for $C_{20}H_{18}N_3O_4ClPt$: C, 40.38; H, 3.05; N, 7.06. Found: C, 39.99; H, 2.80; N, 6.83. FAB-MS: *m*/*z* 495 [M^+], 426 [M^+ − C≡N^{i}Pr]. ^{1}H NMR (CD_3CN): 1.59 (d, 6H, *J* = 6.3 Hz, CH_3), 4.33 (septet, 1H, *J* = 6.5 Hz, CH), 6.92−7.08 (m, 3H), 7.26 (d, 1H, *J* = 7.3 Hz), 7.54 (d, 1H, *J* = 8.1 Hz), 7.63−7.67 (m, 2H), 7.88 (t, 1H, *J* = 8.1 Hz), 7.97 (d, 1H, *J* = 7.9 Hz), 8.18 (t, 1H, *J* = 7.9 Hz), 8.41 (d, 1H, *J* = 5.3 Hz). ^{13}C{^{1}H} NMR (DMSO-d_6): 22.2 (CH_3), 49.8 (CH), 120.2, 120.3, 124.7, 125.6, 126.0, 129.2, 131.8, 136.1, 137.3, 141.4, 142.8, 146.3, 152.4, 154.5, 156.1, 163.6, Pt-*C*N^{i}Pr not resolved. IR (Nujol): *ν* 2209 (C≡N), 1600 (C═N) cm^{-1}.

4(ClO_4): orange solid. Yield: 0.11 g, 80%. Anal. Calcd for $C_{23}H_{22}N_3O_4ClPt$: C, 43.51; H, 3.49; N, 6.62. Found: C, 43.13; H, 3.52; N, 6.50. FAB-MS: *m*/*z* 535 [M^+]. ^{1}H NMR (DMSO-d_6): 1.47−1.51 (m, 4H, CH_2), 1.72−1.75 (m, 2H, CH_2), 1.83−1.93 (m, 2H, CH_2), 2.13−2.14 (m, 2H, CH_2), 4.39 (quintet, 1H, *J* = 4.3 Hz, CH), 7.12−7.21 (m, 3H), 7.68 (d, 1H, *J* = 7.5 Hz), 7.87 (t, 1H, *J* = 6.1 Hz), 8.07 (d, 1H, *J* = 6.9 Hz), 8.19−8.26 (m, 2H), 8.41 (t, 1H, *J* = 7.9 Hz), 8.53 (d, 1H, *J* = 8.0 Hz), 8.77 (d, 1H, *J* = 4.7 Hz). ^{13}C{^{1}H} NMR (DMSO-d_6): 22.6, 24.1, 31.3 (CH_2), 54.9 (CH), 120.1, 120.2, 124.6, 125.6, 125.9, 129.1, 131.7, 136.2, 137.1, 141.3, 142.8, 146.3, 152.2, 154.4, 156.0, 163.5, Pt-*C*NCy not resolved. IR (Nujol): *ν* 2212 (C≡N), 1601 (C═N) cm^{-1}.

[(C^N^N)Pt(C≡NAr′)]PF_6, 5(PF_6). To an orange suspension of [(C^N^N)PtCl] (0.10 g, 0.22 mmol) in acetonitrile (10 mL) was added 2,6-dimethylphenyl (Ar′) isocyanide (0.03 g, 0.23 mmol). The mixture was stirred for 10 min to yield a purple precipitate, which was dissolved into a yellow suspension upon addition of 10 mL of methanol. A yellow solution was obtained by filtration and evaporated to dryness to give a red solid, which was dissolved in methanol, and excess ammonium hexafluorophosphate was added. A purple solid was filtered and recrystallized by vapor diffusion of diethyl ether into an acetonitrile solution to give a purple crystalline solid. Yield: 0.10 g, 66%. Anal. Calcd for $C_{25}H_{20}N_3F_6PPt$: C, 42.74; H, 2.87; N, 5.98. Found: C, 42.39; H, 2.74; N, 6.27. Other spectroscopic characterizations are same as those previously reported for **5**(ClO_4).[13]

[(C^N^N)Pt(CO)]CF_3SO_3, 6(CF_3SO_3). A mixture of [(C^N^N)PtCl] (0.10 g, 0.22 mmol) and silver trifluoromethanesulfonate (0.06 g, 0.23 mmol) in methanol (50 mL) was refluxed for 12 h. The resultant suspension was filtered, and CO gas was bubbled through the yellow filtrate to yield a black-green precipitate, which was isolated and washed with methanol and diethyl ether. Recrystallization from boiling methanol afforded a black-purple crystalline solid. Yield: 0.06 g, 46%. Anal. Calcd for $C_{18}H_{11}N_2F_3SO_4Pt$: C, 35.83; H, 1.84; N, 4.64. Found: C, 36.38; H, 1.71; N, 5.40. FAB-MS: *m*/*z* 454 [M^+], 426 [M^+ − CO]. ^{1}H NMR (CD_3OD): 6.92−7.02 (m, 2H), 7.13 (t, 1H, *J* = 7.6 Hz), 7.39 (d, 1H, *J* = 7.5 Hz), 7.73−7.78 (m, 2H), 7.87 (d, 1H, *J* = 7.8 Hz), 8.04 (t, 1H, *J* = 8.0 Hz), 8.19 (d, 1H, *J* = 7.9 Hz), 8.29 (t, 1H, *J* = 7.8 Hz), 8.78 (d, 1H, *J* = 5.1 Hz). IR (KBr): *ν* 2094 (CO) cm^{-1}.

[{(C^N^N)Pt}$_2$(*μ*-C≡N(CH$_2$)$_3$N≡C)](PF_6)$_2$, 7(PF_6)$_2$. To an orange suspension of [(C^N^N)PtCl] (0.10 g, 0.22 mmol) in acetonitrile (10 mL) at room temperature was added 1,3-diisocyanopropane (0.01 g, 0.11 mmol). Upon stirring, a purple precipitate was filtered and dissolved in methanol, and excess ammonium hexafluorophosphate was added. Recrystallization by slow diffusion of diethyl ether into an acetonitrile solution of the crude product afforded a purple crystalline solid. Yield: 0.11 g, 84%. Anal. Calcd for $C_{37}H_{28}N_6F_{12}P_2Pt_2$: C, 35.93; H, 2.28; N, 6.80. Found: C, 35.54; H, 2.23; N, 6.74. FAB-MS: *m*/*z* 1092 [M^+ + PF_6], 947 [M^+]. ^{1}H NMR (CD_3CN): 2.52 (m, 2H, CH_2CH_2NC), 4.18 (t, 4H, *J* = 5.4 Hz, CH_2NC), 6.73−6.78 (m, 4H), 6.91−6.94 (m, 2H), 7.11−7.14 (m, 2H), 7.27−7.35 (m, 4H), 7.45 (d, 2H, *J* = 8.0 Hz), 7.71−7.81 (m, 4H), 7.96 (t, 2H, *J* = 7.8 Hz), 8.35 (d, 2H, *J* = 5.7 Hz). ^{13}C{^{1}H} NMR (DMSO-d_6): 25.5, 43.4 (CH_2), 119.1, 119.2, 123.7, 124.5, 125.0, 128.0, 130.7, 135.8, 137.8, 139.8, 141.8, 144.4, 151.8, 153.2, 154.4, 162.4, Pt-*C*N not resolved. IR (Nujol): *ν* 2228 (C≡N), 1601 (C═N) cm^{-1}.

Table 1. Crystal Data

	1(ClO_4)·2CH_3CN	**5**(PF_6)·CH_3CN
formula	$C_{25}H_{26}N_5O_4ClPt$	$C_{27}H_{23}N_4F_6PPt$
fw	691.05	743.56
color	yellow	brown
cryst size, mm	0.45 × 0.20 × 0.03	0.35 × 0.10 × 0.05
cryst syst	triclinic	monoclinic
space group	$P\bar{1}$ (No. 2)	$P2_1/c$ (No. 14)
a, Å	7.795(2)	12.692(9)
b, Å	11.271(3)	7.584(4)
c, Å	15.602(5)	28.641(7)
α, deg	97.81(2)	
β, deg	90.07(2)	101.31(3)
γ, deg	94.17(2)	
V, Å^3	1354.4(6)	2703(1)
Z	2	4
D_c, g cm^{-3}	1.694	1.827
μ, cm^{-1}	52.97	52.95
F(000)	676	1440
$2\theta_{max}$, deg	50	50
no. unique data	4782	5149
no. obsd data for $I > 3\sigma(I)$	4111	2938
no. variables	322	319
R^a	0.034	0.040
$R_w{}^b$	0.051	0.050
residual *ρ*, e Å^{-3}	+1.02, −0.82	+1.09, −0.75

^{a} $R = \sum||F_o| - |F_c||/\sum|F_o|$. ^{b} $R_w = [\sum w(|F_o| - |F_c|)^2/\sum w|F_o|^2]^{1/2}$.

X-ray Crystallography. Crystals of **1**(ClO_4)·2CH_3CN and **5**(PF_6)·CH_3CN were grown by slow diffusion of diethyl ether into acetonitrile solutions. Crystal data and details of data collection and refinement are summarized in Table 1; full crystallographic data are provided in the Supporting Information.

Diffraction experiments were performed at 301 K on a Rigaku AFC7R diffractometer with graphite-monochromatized Mo Kα radiation (*λ* = 0.71073 Å) using *ω*−2*θ* scans. The structures were solved by Patterson and Fourier methods (PATTY)[18] and refined by full-matrix least-squares using the software package TeXsan[19] on a Silicon Graphics Indy com-

(18) PATTY: Beurskens, P. R.; Admiraal, G.; Bosman, W. P.; Garcia-Granda, S.; Gould, R. O.; Smits, J. M. M.; Smykalla, C. *The DIRDIF program system*, Technical Report of the Crystallography Laboratory; University of Nijmegen: The Netherlands, 1992.

(19) *TeXsan*: Crystal Structure Analysis Package; Molecular Structure Corporation: The Woodlands, TX, 1985 and 1992.

Downloaded by CARLI CONSORTIUM on June 29, 2009
Published on December 11, 2001 on http://pubs.acs.org | doi: 10.1021/om0106276

Scheme 1

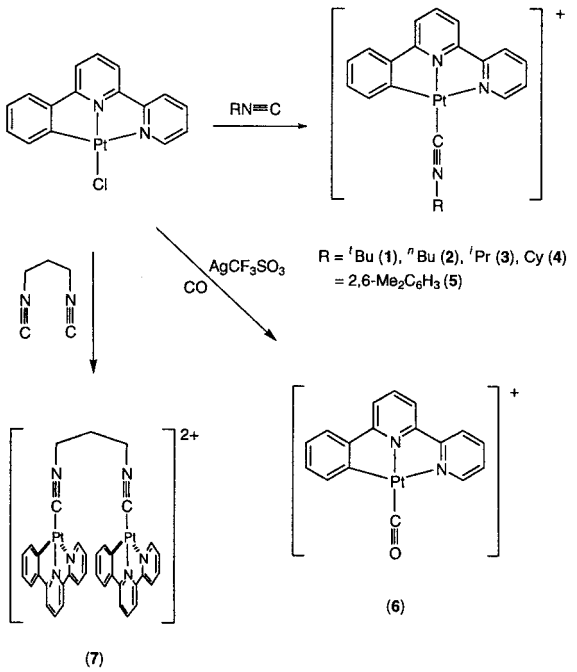

puter. For **1**$(ClO_4)\cdot 2CH_3CN$, a crystallographic asymmetric unit consists of one molecule. The O atoms of the anion were disordered and were placed at seven positions with O(1), O(2), O(2′), O(3), O(3′), O(4), and O(4′) having occupation numbers of 1.0, 0.74, 0.26, 0.72, 0.28, 0.66, and 0.34, respectively. In the least-squares refinement, 33 non-H atoms were refined anisotropically, the 6 O atoms with partial occupancy were refined isotropically, and 26 H atoms at calculated positions with thermal parameters equal to 1.3 times that of the attached C atoms were not refined. For **5**$(PF_6)\cdot CH_3CN$, a crystallographic asymmetric unit consists of one molecule. The F atoms of the anion were disordered and were placed at nine positions with F(1), F(2), F(2′), F(3), F(4), F(5), F(5′), F(6), and F(6′) having occupation numbers of 1.0, 0.55, 0.35, 0.84, 1.0, 0.53, 0.42, 0.76, and 0.55, respectively. In the least-squares refinement, 30 non-H atoms were refined anisotropically, the F atoms and atoms of the solvent molecule were refined isotropically, and 23 H atoms at calculated positions were not refined.

Results and Discussion

Synthesis and Characterization. The facile displacement of the chloride group from [(C^N^N)PtCl] by excess isocyanide yielded complexes **1**−**5** in moderate to high yields (Scheme 1). By using the 1,3-diisocyanopropane ligand, we have prepared the binuclear species **7** with two [(C^N^N)Pt] moieties. Treatment of [(C^N^N)PtCl] with $AgCF_3SO_3$ followed by bubbling with CO gas yielded the carbonyl derivative, **6**. All complexes are air- and moisture-stable at room temperature. Except for **1**, these solids display intense colors ranging from orange, to red, to purple. Yellow or orange solutions are obtained when these solids are dissolved in acetonitrile. The FAB mass spectra of **1**−**6** reveal a cluster corresponding to $[M^+]$, while **7** shows a cluster around *m*/*z* 1092, the intensities of which are comparable to the calculated isotopic pattern for $[M^+ + PF_6]$. The binuclear complex **7**, with two [(C^N^N)PtC≡N] motifs linked through a propyl spacer, was designed to encourage metal−metal and/or ligand-ligand interactions. The characteristic IR absorptions ν(C≡N) for isocyanide complexes appear in the range 2169−2228 cm^{-1}, which are comparable to that of Pt(II) isocyanide analogues $[Pt(CNCH_3)_3Br]PF_6$ (2286 cm^{-1}),[20] $[PtCl_2\{CN(CH_2)_3Si(OC_2H_5)_3\}_2]$ (2263 cm^{-1}),[21] and *trans*-$[PtI_2\{CNC_6H_2$-^{i}Pr$_2$-2,6-$(C_5H_4$N-4)-4$\}_2]$ (2188 cm^{-1}).[22] The CO stretching frequency of **6**(CF_3SO_3) in KBr disk is at 2094 cm^{-1}, which is larger than that of 2036 cm^{-1} for the related [(C^N^C)Pt(CO)] complex.[14] All ^{1}H and ^{13}C NMR spectra of isocyanide complexes in this work are clearly resolved except for the Pt-*C*≡NR resonances. The carbonyl derivative **6** is stable in the solid state, but the CO group can be displaced by coordinating solvents in solution.

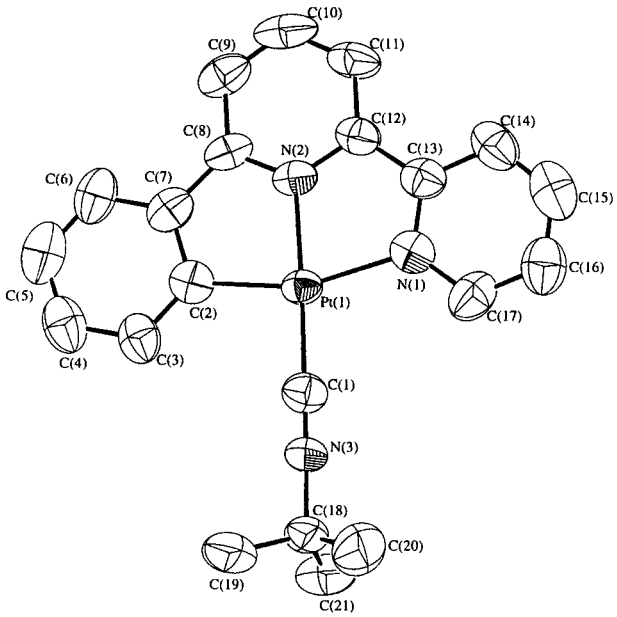

Figure 2. Perspective view of the cation in **1**$(ClO_4)\cdot 2CH_3CN$ (50% probability ellipsoids).

Crystal Structures. X-ray structural determinations of **1**$(ClO_4)\cdot 2CH_3CN$ and **5**$(PF_6)\cdot CH_3CN$ have been performed (Figures 2 and 3a, respectively); selected bond lengths and angles are listed in Table 2. Each of the complex cations consists of a platinum atom residing in a distorted square-planar environment and coordinated by a tridentate C^N^N ligand and a ^{t}Bu- or Ar′-substituted isocyanide group. The bite angle of the tridentate C^N^N ligand deviates substantially from 180° (N(1)−Pt(1)−C(2) for **1** and **5**: 159.7(3)° and 160.8(4)°, respectively) and is similar to that in previously reported derivatives, namely, $[(C^N^N)PtPPh_3]ClO_4$ (157.9(4)°)[9c] and [(C^N^N)Pt{C(NH^{t}Bu)(NHCH$_2$Ph)}]ClO_4 (159.2(2)°).[13] The isocyanide platinum−carbon bond lengths of 1.936(8) and 1.90(1) Å for **1** and **5** are comparable to that in $[PtH(^tBu_2P(CH_2)_2P^tBu_2)(CNAr')]PF_6$ (1.947(8) Å)[23] and $[Pt(CNC_6H_2$-2,4-^{t}Bu$_2$-6-Me$)_2Cl]_2$ (mean 1.95 Å).[24] Bond angles of C(1)−N(3)−C(18) in **1** and **5** (177.5(9)° and 176(1)°, respectively) are close to linearity and compare favorably with the values found in *trans*-$[PdCl(CNAr')_2\{P[C_6H_3(OMe)_2]_3\}]PF_6$ (173.6(4)°

(20) Miller, J. S.; Balch, A. L. *Inorg. Chem.* **1972**, *11*, 2069.
(21) Gao, H.; Angelici, R. J. *Organometallics* **1999**, *18*, 989.
(22) Mayr, A.; Guo, J. *Inorg. Chem.* **1999**, *38*, 921.
(23) Tanase, T.; Ukaji, H.; Kudo, Y.; Ohno, M.; Kobayashi, K.; Yamamoto, Y. *Organometallics* **1994**, *13*, 1374.
(24) Yamamoto, Y.; Takahashi, K.; Yamazaki, H. *Chem. Lett.* **1985**, 201.

Downloaded by CARLI CONSORTIUM on June 29, 2009
Published on December 11, 2001 on http://pubs.acs.org | doi: 10.1021/om0106276

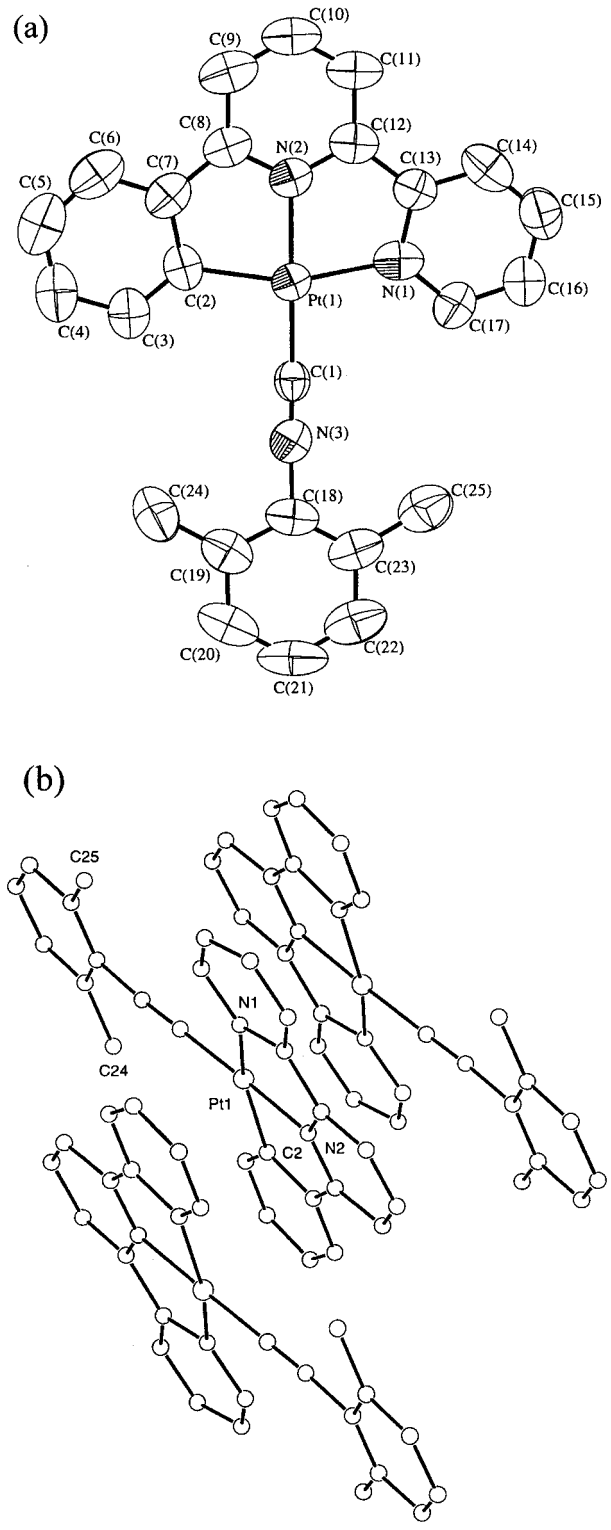

Figure 3. (a) Perspective view of the cation in **5**$(PF_6)\cdot CH_3CN$ (50% probability ellipsoids). (b) Crystal packing diagram showing metal−metal and $\pi-\pi$ interactions.

and 177.8(4)°)[25] and *cis*-$[PtCl_2(CNEt)(PEt_2Ph)]$ (172(3)°).[26a] Bond distances of C(1)−N(3) (1.13(1) Å for **1** and 1.15(1) Å for **5**) are similar to the carbon−nitrogen triple bonds reported in *cis*-$[PtCl_2(CNPh)_2]$ (1.19(2) and 1.14(3) Å)[26b] and $[Rh_2(1,3\text{-diisocyanopropane})_4](BPh_4)_2$ (1.14(1) Å).[27]

Table 2. Selected Bond Lengths (Å) and Angles (deg)

Complex **1**$(ClO_4)\cdot 2CH_3CN$			
Pt(1)−C(1)	1.936(8)	C(1)−N(3)	1.13(1)
Pt(1)−N(1)	2.095(7)	N(3)−C(18)	1.47(1)
Pt(1)−C(2)	2.036(8)	C(9)−C(10)	1.36(1)
Pt(1)−N(2)	1.988(6)	C(18)−C(21)	1.50(1)
Pt(1)−C(1)−N(3)	179.8(8)	N(3)−C(18)−C(20)	108.3(8)
C(1)−N(3)−C(18)	177.5(9)	N(1)−Pt(1)−C(1)	102.9(3)
N(1)−Pt(1)−N(2)	78.8(3)	N(1)−Pt(1)−C(2)	159.7(3)
N(2)−Pt(1)−C(1)	178.1(3)		
Complex **5**$(PF_6)\cdot CH_3CN$			
Pt(1)−C(1)	1.90(1)	C(1)−N(3)	1.15(1)
Pt(1)−N(1)	2.06(1)	N(3)−C(18)	1.45(1)
Pt(1)−C(2)	2.06(1)	C(14)−C(15)	1.35(2)
Pt(1)−N(2)	1.998(8)	C(19)−C(24)	1.50(2)
Pt(1)−C(1)−N(3)	178.1(9)	N(3)−C(18)−C(19)	116(1)
C(1)−N(3)−C(18)	176(1)	N(1)−Pt(1)−C(1)	99.2(4)
N(1)−Pt(1)−N(2)	80.2(4)	N(1)−Pt(1)−C(2)	160.8(4)
N(2)−Pt(1)−C(1)	178.1(4)		

Effects of different substituents on the isocyanide ligand upon the stacking interactions of the complex cations are demonstrated. In the crystal packing diagram of **1**, the cations are orientated in a head-to-tail fashion and form a continuous stack with no metal−metal communication (average Pt−Pt distance of 4.74 Å). A dihedral angle of 3.2° is observed in **5** between the aryl moiety of the C≡N(2,6-$Me_2C_6H_3$) isocyanide ligand and the mean plane of the [(C^N^N)Pt] moiety. Both **1** and **5** show interplanar separations of ca. 3.4−3.6 Å between C^N^N ligands, which are sufficiently close for $\pi-\pi$ interactions.[28] As shown in Figure 3b, the cations of **5** stack in pairs in a head-to-tail style with alternating short/long Pt−Pt distances (3.3831(9) and 4.6030(9) Å, respectively). The former distance is comparable to that in $[\{Pt(tpy)\}_2(\mu\text{-pz})](ClO_4)_3$ (3.432(3) Å)[29] and the intermolecular Pt−Pt contacts of 3.48 Å in *cis*-$[PtCl_2(CNPh)_2]$,[26b] which suggests some degree of metal−metal interactions. This is in contrast to the crystal lattice of the related analogue [(C^N^C)Pt(C≡NAr′)];[15] a larger dihedral angle (mean 28.6°) between the ring of the C≡NAr′ ligand and the Pt(C^N^C) plane is observed, and no close Pt−Pt contact (<4 Å) is evident though intermolecular $\pi-\pi$ stacking between the phenyl ring and the Pt(C^N^C) fragment is separated by 3.39 Å. Such intermolecular Pt−Pt interaction in **5** imposes notable perturbation to the emission properties (see below).

Absorption Spectroscopy. The UV−visible spectral data of complexes **1**−**7** in acetonitrile and [(C^N^C)Pt(CO)] in dichloromethane are listed in Table 3 (see Figure 4 for **2**). Like for previously described Pt(II) complexes,[8,9a−c] their absorption spectra obey Beer's law in the concentration range 10^{-6} to 10^{-3} mol dm^{-3}. In the high-energy region, the vibronically structured absorption centered at λ_{max} 340 nm ($\epsilon \approx 10^4$ dm^3 mol^{-1} cm^{-1}) for **1**−**7** is assigned to the intraligand ^{1}IL ($\pi \rightarrow \pi^*$) transition of the C^N^N group, while the moder-

(25) Yamamoto, Y.; Arima, F. *J. Chem. Soc., Dalton Trans.* **1996**, 1815.

(26) (a) Jovanović, B.; Manojlović-Muir, Lj. *J. Chem. Soc., Dalton Trans.* **1972**, 1176. (b) Jovanović, B.; Manojlović-Muir, Lj.; Muir, K. W. *J. Chem. Soc., Dalton Trans.* **1972**, 1178.

(27) Mann, K. R.; Thich, J. A.; Bell, R. A.; Coyle, C. L.; Gray, H. B. *Inorg. Chem.* **1980**, *19*, 2462.

(28) Hunter, C. A.; Sanders, J. K. M. *J. Am. Chem. Soc.* **1990**, *112*, 5525.

(29) Bailey, J. A.; Gray, H. B. *Acta Crystallogr.* **1992**, *C48*, 1420.

Table 3. UV−Visible Absorption Data in Acetonitrile at 298 K unless Otherwise Stated

complex	λ_{max}/nm (ϵ/dm^3 mol^{-1} cm^{-1})
1(ClO_4)	250 (27800), 264 (26800), 333 (12800), 348 (12000), 398 (sh, 1000)
2(ClO_4)	250 (35600), 263 (34900), 324 (14900), 337 (16800), 350 (15000), 406 (770), 511 (120)
3(ClO_4)	250 (29900), 263 (28900), 327 (12800), 345 (12300), 411 (510), 499 (50)
4(ClO_4)	250 (30000), 263 (28700), 325 (12800), 335 (13400), 348 (12300), 400 (640), 418 (540), 499 (65)
5(PF_6)	249 (37300), 263 (34600), 334 (15000), 350 (14500), 402 (650), 419 (540), 497 (40)
6(CF_3SO_3)	240 (sh, 26600), 250 (27900), 265 (sh, 25000), 323 (11500), 351 (12000), 425 (sh, 1000), 505 (230)
7(PF_6)$_2$	252 (53900), 335 (19600), 358 (sh, 13600), 401 (3900), 478 (830), 511 (370)
[(C^N^C)Pt(CO)]	273 (20400), 280 (sh, 17900), 336 (10900), 351 (10300), 440 (sh, 450), 510 (sh, 70)[a]

[a] Measured in dichloromethane.

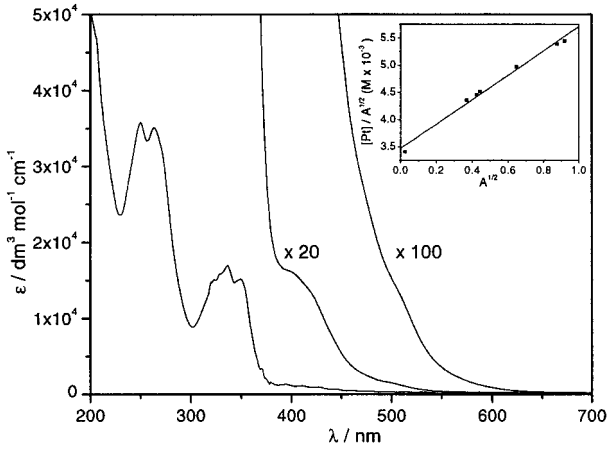

Figure 4. UV−vis absorption spectrum of **2** in acetonitrile at 298 K (inset: dimerization plot of [Pt]/$A^{1/2}$ versus $A^{1/2}$ for **2** at 511 nm in acetonitrile).

ately intense low-energy bands with λ_{max} in the range 390−430 nm ($\epsilon \approx 5 \times 10^2$ dm^3 mol^{-1} cm^{-1}) are assigned to ^{1}MLCT [(5d)Pt → π*(C^N^N)] transitions. At concentrations higher than 10^{-3} mol dm^{-3}, a shoulder at λ_{max} 511 nm ($\epsilon \approx 120$ dm^3 mol^{-1} cm^{-1}) for complex **2** is observed at room temperature (Figure 4). This absorption band is too low in energy to be assigned to an intraligand ^{3}IL ($\pi \rightarrow \pi$*) transition. An assignment of ^{3}MLCT [(5d)Pt → π*(C^N^N)] is not preferred since the ^{3}MLCT transition of [Pt(^{t}Bu$_3$tpy)Cl]$^+$ (^{t}Bu$_3$tpy = 4,4′,4″-tri-*tert*-butyl-2,2′:6′,2″-terpyridine) occurs at λ_{max} 465 nm.[30] The π* orbital of the C^N^N ligand is higher in energy than that of ^{t}Bu$_3$tpy, and hence the ^{3}MLCT transitions of complexes **1**−**7** are envisioned to occur at λ < 465 nm.

A nonlinear plot of absorbance at 511 nm against the concentration of **2**(ClO_4) in acetonitrile demonstrates that this absorption band does not obey the Beer−Lambert law. A similar finding for a concentrated *N*,*N*-dimethylformamide (DMF) solution of [Pt(tpy)Cl]$^+$ was reported previously by Gray and co-workers,[6d] namely, that dimerization of [Pt(tpy)Cl]$^+$ to afford [Pt(tpy)Cl]$_2^{2+}$ was responsible for a low-energy absorption at 470 nm

(30) Lai, S. W.; Chan, M. C. W.; Cheung, K. K.; Che, C. M. *Inorg. Chem.* **1999**, *38*, 4262.

Table 4. Fluid Emission Data (concentration 5 × 10^{-5} M except 7 (1.5 × 10^{-4} M); λ_{ex} 350 nm)

complex	298 K:[a] λ_{max}/nm; τ_o/μs; ϕ_o	77 K:[c] λ_{max}/nm
1(ClO_4)	533; 1.12; 0.11	505 (max), 538, 581 (sh)
2(ClO_4)	529; 1.70; 0.06	502 (max), 539, 587
3(ClO_4)	529; 2.03; 0.07	502 (max), 538, 583
4(ClO_4)	530; 2.29; 0.075	501 (max), 538, 580
5(PF_6)	528; 2.19; 0.083	502 (max), 538, 580
6(CF_3SO_3)	526, 546 (sh); 2.93; 0.036	580[d]
7(PF_6)$_2$	555 (sh), 630; 3.27; 5×10^{-3}	600 (sh), 744
[(C^N^C)Pt(CO)]	528, 563; 0.16; 0.012[b]	529, 561[e]

[a] Measured in acetonitrile unless otherwise stated. [b] Measured in dichloromethane. [c] Measured in butyronitrile unless otherwise stated; additional emission band(s) observed in ≥10^{-3} M glasses at λ_{max} 625 (**1**); 615, 739 (**2**); 600 (**3**); 625, 710 (**4**); 711 (**5**); and 714 nm (**6**), respectively. [d] Measured in 1:4:5 DMF/MeOH/EtOH. [e] Measured in 1:5 MeOH/EtOH.

attributable to a ^{1}(dσ* → π*) transition. From studies of the concentration dependence upon the UV absorbance, an equation for determining the ϵ value and dimerization constant K is

$$[Pt]/A^{1/2} = 1/(\epsilon K)^{1/2} + (2/\epsilon)(A^{1/2})$$

where [Pt] is the total Pt concentration; A is the absorbance; ϵ is the extinction coefficient; and K is the dimerization constant.

A dimerization plot of [Pt]/$A^{1/2}$ versus $A^{1/2}$ for **2**(ClO_4) in the concentration range from 8.4×10^{-5} to 5.0×10^{-3} mol dm^{-3} at λ_{max} 511 nm in acetonitrile is shown as the inset of Figure 4. A straight line with slope of (2/ϵ) and y-intercept of $1/(\epsilon K)^{1/2}$ confirms the assignment of this low-energy absorption band to arise from the [(C^N^N)-Pt(C≡N^{n}Bu)]$_2^{2+}$ species.

The value of ϵ is calculated to be about 900 dm^3 mol^{-1} cm^{-1}, which is comparable to that of [Pt(tpy)Cl]$^+$ in DMF[6d] at 470 nm (~1000 dm^3 mol^{-1} cm^{-1}). The equilibrium constant K determined in this work is 93 dm^3 mol^{-1}, which is significantly smaller than that for [Pt(tpy)Cl]$^+$ in DMF (~3000 dm^3 mol^{-1}). The large difference between these equilibrium constants may be due to the different solvents used in the measurements (CH_3CN vs DMF). Similarly, a concentrated solution of the carbonyl derivative **6**(CF_3SO_3) shows a weak band at 505 nm (ϵ 230 dm^3 mol^{-1} cm^{-1}), which is tentatively assigned to a MMLCT [dσ*(Pt−Pt) → π*(C^N^N)] absorption.

We envisaged that the binuclear complex **7**(PF_6)$_2$ would yield two closely interacting [(C^N^N)Pt] groups via intermolecular metal−metal and/or π−π contacts. However, even though a similar absorption at λ > 500 nm was observed like for concentrated acetonitrile solutions of **2**(ClO_4), there is no distinct absorption band similar to the ^{1}[5dσ* → 6pσ*] transition of [Pt$_2$(μ-$P_2O_5H_2$)$_4$]$^{4-}$ [3c] in this spectral region.

Solution Luminescence Spectroscopy. All complexes in this work are emissive in solution at room temperature (Table 4). With reference to earlier work,[8,9c,d,13] the structureless emissions of complexes **1**−**6** (at $\lambda_{max} \approx 529$ nm) in acetonitrile are assigned as ^{3}MLCT in nature. The binuclear complex **7** shows a broad emission at 630 nm, which can be attributed to

Downloaded by CARLI CONSORTIUM on June 29, 2009
Published on December 11, 2001 on http://pubs.acs.org | doi: 10.1021/om0106276

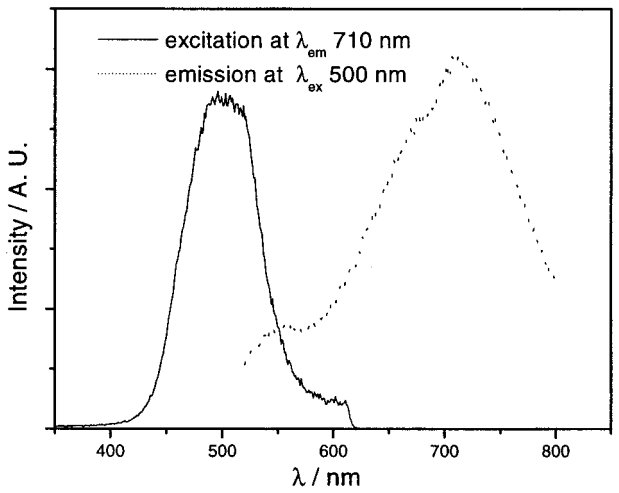

Figure 5. Normalized excitation and emission spectra (λ_{em} 710 nm and λ_{ex} 500 nm, respectively) of **4** in acetonitrile at 298 K with concentration $\geq 7 \times 10^{-3}$ M.

Downloaded by CARLI CONSORTIUM on June 29, 2009
Published on December 11, 2001 on http://pubs.acs.org | doi: 10.1021/om0106276

an excimeric intraligand (^{3}IL) excited state and which resembles the 626 nm emission observed in a glassy solution of [{(C^N^N)Pd}$_2$(μ-dppm)]$^{2+}$.[31] Like other established cyclometalated platinum(II) complexes,[8,13] self-quenching of the ^{3}MLCT emission for complex concentrations in the 10^{-5} to 10^{-3} mol dm^{-3} range is evident for complexes **1**−**7** at 298 K in CH_3CN solution (e.g., $k_q = 2.3 \times 10^9$, 3.5×10^9, and 2.4×10^9 dm^3 mol^{-1} s^{-1} for **1**, **4**, and **5**, respectively), where in each case a linear plot of $1/\tau$ versus complex concentration was obtained. Lifetimes ranging from 1.12 (for **1**) up to 3.27 (for **7**) μs are detected. High-emission quantum yields in the range 0.060−0.11 for **1**−**5** may be rationalized by the strong ligand field of RN≡C, which increases the energy of ligand-field excited states so that radiationless decay is less prevalent.

At concentrations $\geq 7 \times 10^{-3}$ mol dm^{-3}, the emission spectrum of **4**(ClO_4) in acetonitrile (λ_{ex} 500 nm) displays a broad band at 710 nm (dotted line in Figure 5). When monitoring the emission wavelength at 710 nm, the excitation spectrum exhibits a pronounced maximum at ∼500 nm (solid line in Figure 5), which is similar in energy to the proposed singlet MMLCT (dσ* → π*) absorption discussed in the previous section. At concentration of 4×10^{-3} mol dm^{-3}, in addition to emission at 710 nm, an emission band at 550 nm is also observed for **4**(ClO_4) in acetonitrile. The latter occurs at an energy similar to the ^{3}MLCT emission of previously reported monomeric (C^N^N)Pt derivatives, while the emission band at 710 nm is too low in energy to be assigned to π−π excimeric emission of C^N^N ligands (λ_{max} 600−650 nm). Thus the emission at 710 nm is presumably associated with the metal−metal interaction of the dimeric [(C^N^N)Pt(C≡NCy)]$_2^{2+}$ species and tentatively assigned to the triplet MMLCT (π* → dσ*) emission with reference to previous work on the binuclear compound [{Pt(tpy)}$_2$(μ-dpf)]$^{3+}$ (dpf = diphenylformamidine) (λ_{em} 670 nm)[7c] and [Pt(tpy)Cl]$^+$ (λ_{em} 740 nm)[6d] in glassy solution at 77 K. The absorption at λ ∼500 nm is assigned to a singlet MMLCT transition of the ground-state [(C^N^N)Pt(C≡NCy)]$_2^{2+}$ species, which exhibits

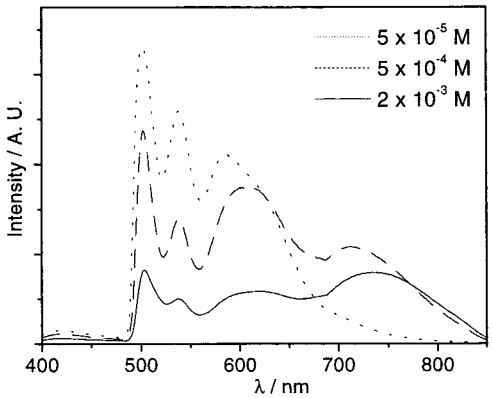

Figure 6. Emission spectra of **2** in the concentration range 5×10^{-5} to 2×10^{-3} M in glassy butyronitrile solution at 77 K (λ_{ex} 350 nm).

triplet MMLCT ^{3}(π* → dσ*) emission at 710 nm. At concentrations $\geq 5 \times 10^{-4}$ mol dm^{-3}, the emission spectrum of [(C^N^N)Pt(CO)]$^+$ (**6**) in acetonitrile shows a red emission at 707 nm at the expense of the yellow band at λ_{max} 526 nm. Monitoring the emission wavelength at 707 nm, the excitation spectrum displays a well-defined singlet MMLCT (dσ* → π*) absorption at 540 nm. Nevertheless, in a concentrated solution of [(C^N^C)Pt(CO)], no such low-energy MMLCT absorption or emission is observed.

The emissive behavior of **1**−**7** at 77 K in glassy solutions has been examined (Table 4). The emissions are sensitive to the complex concentration for **1**−**6** in the range 10^{-3} to 10^{-5} mol dm^{-3}. At a complex concentration < 10^{-5} mol dm^{-3}, the emission spectrum is vibronically structured with peak maxima at λ_{max} ∼502 nm for **1**−**5** (λ_{max} 580 nm for **6**); the vibrational progressions of ca. 1300 cm^{-1} correspond to the skeletal stretching of the free HC^N^N ligand. The most intense vibronic component is $v' = 0$ to $v'' = 0$, indicating that the emission is ^{3}MLCT in nature. At higher concentrations ($\geq 10^{-4}$ mol dm^{-3}), the emission profile changes dramatically. A new red emission band centered at 600−625 nm (for **1**−**4**) develops at the expense of the yellow band at λ_{max} 502 nm (see Figure 6 for **2**). The former are tentatively ascribed to an excimeric intraligand excited state arising from weak π-stacking interactions of the C^N^N ligand, by reference to previous reports on π−π excimeric emission of [Pt(tpy)Cl]$^+$ (650 nm in 5:5:1 EtOH/MeOH/DMF),[6d] [Pt(^{t}Bu$_3$tpy)Cl]$^+$ (625 nm in 1:1 MeOH/EtOH),[30] and [Pd(C^N^N)PPh$_3$]$^+$ (626 nm in 1:1 MeOH/EtOH).[31] Furthermore, low-energy emission bands at λ_{max} 739 (Figure 6) and 710 nm also appear for **2** and **4**, respectively. The energies of these bands are very similar to the 740 nm glassy emission of [Pt(tpy)Cl]$^+$ at 77 K and can be attributed to MMLCT excited states resulting from oligomerization of Pt(II) centers in glassy solutions.[6b,d] For **5**(PF_6) and **6**(CF_3SO_3), only red emission bands at λ_{max} 711 and 714 nm were observed, respectively, for increases in complex concentration, and these are similarly assigned to MMLCT transitions. The binuclear complex **7**(PF_6)$_2$ exhibits a low-energy emission at 744 nm in a 77 K butyronitrile glass solution at 10^{-4} mol dm^{-3}, and a ^{3}MMLCT excited state is similarly proposed. For [(C^N^C)Pt(CO)] in 77 K methanol/ethanol (1:5, v/v) glass, no red emission is detected upon increasing the complex concentration from 1×10^{-5} to 1×10^{-3} mol dm^{-3}.

(31) Lai, S. W.; Cheung, T. C.; Chan, M. C. W.; Cheung, K. K.; Peng, S. M.; Che, C. M. *Inorg. Chem.* **2000**, *39*, 255.

Table 5. Solid-State Emission Data (λ_{ex} 350 nm)

solid state	298 K: λ_{max}/nm; τ_o/μs	77 K: λ_{max}/nm
1(ClO_4)	579, 612 (sh); 2.60	547 (sh), 568 (max), 610 (sh)
2(ClO_4)	748; 0.20	798
3(ClO_4)	722; 0.34	775
4(ClO_4)	625; 1.08	640
5(PF_6)	701; 0.17	776
6(CF_3SO_3)	726; ≤0.1	813
7$(PF_6)_2$	711; 0.27	744
[(C^N^C)Pt(CO)]	583; 0.836	554, 576 (max), 629, 670 (sh), 695 (sh)

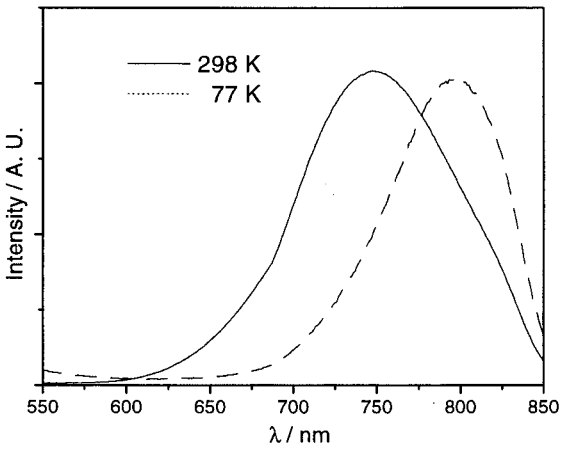

Figure 7. Solid-state emission spectra of **2**(ClO_4) at 77 and 298 K (λ_{ex} 350 nm, normalized intensities).

Solid-State Spectroscopy. The solid-state luminescence data for complexes **1**−**7** are listed in Table 5. The emissions are highly dependent on the R substituent of the isocyanide ligand. For example, the yellow *tert*-butyl isocyanide derivative **1**(ClO_4) displays poorly resolved vibronic structure at λ_{max} 579 nm which slightly blue-shifts at 77 K. These emissions are attributed to ^{3}MLCT excited states with excimeric character due to weak C^N^N $\pi-\pi$ interactions. This correlates to the stacking of C^N^N ligands evident in the crystal lattice of **1**(ClO_4) (range 3.4−3.6 Å) with no metal−metal interaction (Pt−Pt distance 4.74 Å). The orange cyclohexyl isocyanide complex **4**(ClO_4) exhibits a broad structureless emission at λ_{max} 625 nm at room temperature, but red-shifts to 640 nm with reduced bandwidth. This is reminiscent of an excimeric ^{3}IL transition resulting from π-stacking of C^N^N ligands in the [Pt(C^N^N)PPh_3]ClO_4 solid.[9c] The strikingly intense red to purple colors of **2**(ClO_4), **3**(ClO_4), **5**(PF_6), and **7**$(PF_6)_2$ in their solid state are attributed to the propensity of these square-planar Pt(II) species, like the established diimine relatives, to undergo solid-state intermolecular metal−metal and ligand−ligand interactions which give low-energy [d$\sigma^* \rightarrow \pi^*$] transitions.[5] At room temperature, these microcrystalline samples show a structureless emission with λ_{max} in the range 701−748 nm. Upon cooling to 77 K, the bandwidths of the emissions are reduced and the emission maxima are red-shifted to 744−798 nm (Figure 7 for **2**). This can be rationalized by the shortening of intermolecular Pt−Pt and $\pi-\pi$ separations in the crystal lattice at reduced temperatures, which results in ^{3}[dσ^*, π^*] emissions of lower energies.[5f] The solid-state emission band at 298 K for the carbonyl derivative, **6**(CF_3SO_3), is observed at λ_{max} 726 nm and is red-shifted to 813 nm at 77 K; a ^{3}MMLCT excited state is tentatively assigned. In contrast, the neutral complex [(C^N^C)Pt(CO)] exhibits the solid-state emissions with λ_{max} 583 nm at 298 K and λ_{max} 576 nm at 77 K, which are attributed to an excimeric ligand-to-ligand excited state. This correlates the crystal lattice of [(C^N^C)Pt(CO)][14] that shows only $\pi-\pi$ stacking interactions, but no close intermolecular metal−metal contacts are evident.

General Remarks

In recent years, interest in luminescent platinum(II) complexes, particularly those with aromatic diimine and cyclometalated ligands, has proliferated.[1,2,5−9] Like tris(2,2′-bipyridine)ruthenium(II) and its derivatives, this class of compounds has found applications in photochemical devices[3] and as chemical sensors.[1,2] They are air- and moisture-stable and are readily prepared by reacting a Pt(II) precursor with the appropriate organic ligand. More importantly, their photoluminescent properties can be systematically tuned through modification of the diimine/cyclometalated ligands. Their square-planar geometry confers different photophysical and photochemical properties from that of the octahedral $[Ru^{II}(bpy)_3]^{2+}$ complex; for example, they are more likely to undergo substrate-binding reactions in both the ground and MLCT excited states. However, the MLCT absorptions of monomeric platinum(II) complexes bearing aromatic diimines usually occur at higher energies[5−7,32] than that of the $[Ru^{II}(bpy)_3]^{2+}$ system. This is clearly not desirable in the context of developing photocatalysts for solar energy reactions. One strategy to red-shift the MLCT transition of Pt(II) derivatives is through metal−metal and ligand−ligand interactions. As stated in the Introduction, platinum(II) diimine solids exhibit unusual color and low-energy emissions arising from metal−metal-to-ligand charge transfer (MMLCT) excited states. A number of binuclear platinum(II) diimine complexes exhibiting Pt−Pt contacts of less than 3 Å have recently been reported.[7a,c] Their emissions range from 650 to 750 nm[7c] and are distinctly red-shifted from the ^{3}MLCT of monomeric congeners. Nevertheless, their absorption spectra do not exhibit distinct singlet MMLCT transitions in the visible region. In this work, by recording the excitation spectrum, we have observed a well-resolved absorption band at 500 nm which is substantially red-shifted from the absorption spectrum of monomeric derivatives. There is no alternative assignment to this absorption other than the ^{1}MMLCT transition. Previous studies on phosphine analogues such as $[(C^N^N)PtPPh_3]^+$ [9c] and $[\{(C^N^N)Pt\}_2(\mu\text{-dppm})]^{2+}$ [8,9c] failed to reveal similar excitation spectra. The employment of less bulky π-acceptor ligands such as isocyanide and CO in this work favors metal−metal interactions and accounts for the observation of this low-energy ^{1}MMLCT transition. However, complex **7** with two [Pt(C^N^N)] units connected by a bridging diisocyanide does not display a distinct MMLCT absorption band in CH_3CN. In solution, we suggest that **7** is conformationally nonrigid and the following equilibrium takes place (Figure 8). We have also found that unlike

(32) (a) Paw, W.; Cummings, S. D.; Mansour, M. A.; Connick, W. B.; Geiger, D. K.; Eisenberg, R. *Coord. Chem. Rev.* **1998**, *171*, 125. (b) Connick, W. B.; Miskowski, V. M.; Houlding, V. H.; Gray, H. B. *Inorg. Chem.* **2000**, *39*, 2585.

Downloaded by CARLI CONSORTIUM on June 29, 2009
Published on December 11, 2001 on http://pubs.acs.org | doi: 10.1021/om0106276

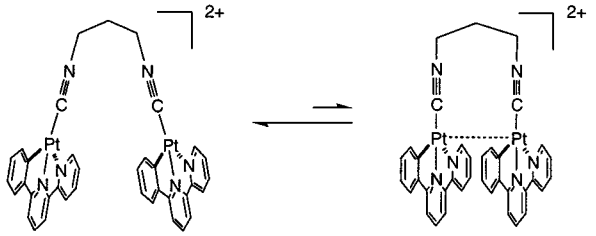

Figure 8.

the [(C^N^N)Pt] analogues, the isostructural [(C^N^C)-Pt(CO)] and [(C^N^C)Pt(C≡NAr′)] complexes do not show emission and absorption bands via excitation spectroscopy that could be assigned to MMLCT excited states. The major difference between the [(C^N^N)Pt-(C≡NAr′)]$^+$ and [(C^N^C)Pt(C≡NAr′)] lies in the electronic charge on the metal complexes, which is higher for the former. This information should be considered for the future design of platinum complexes that display intense low-energy MMLCT absorptions in fluid solution at ambient temperature.

Acknowledgment. We are grateful for financial support from The University of Hong Kong and the Research Grants Council of the Hong Kong SAR, China [HKU 7298/99P].

Supporting Information Available: Listings of crystal data, atomic coordinates, calculated coordinates, anisotropic displacement parameters, bond lengths and angles, and intermolecular nonbonded contacts for **1**(ClO_4)·2CH_3CN and **5**(PF_6)·CH_3CN. This material is available free of charge via the Internet at http://pubs.acs.org.

OM0106276

Downloaded by CARLI CONSORTIUM on June 29, 2009
Published on December 11, 2001 on http://pubs.acs.org | doi: 10.1021/om0106276